

Tumor Microenvironment of Metastasis in Human Breast Carcinoma: A Potential Prognostic Marker Linked to Hematogenous Dissemination

Brian D. Robinson,¹ Gabriel L. Sica,¹ Yi-Fang Liu,¹ Thomas E. Rohan,² Frank B. Gertler,⁴ John S. Condeelis,³ and Joan G. Jones¹

Abstract Purpose: Multiphoton-based intravital imaging has shown that invasive carcinoma cells in mouse and rat mammary tumors intravasate when associated with perivascular macrophages, identifying a potential tumor microenvironment of metastasis (TMEM). We define TMEM as the tripartite arrangement of an invasive carcinoma cell, a macrophage, and an endothelial cell. The aim of this study was to determine if TMEM density in human breast carcinoma samples predicts the development of systemic, hematogenous metastases.

Experimental Design: A case-control study of 30 patients who developed metastatic breast cancer and 30 patients without metastatic disease was done. Cases were matched to controls based on currently used prognostic criteria. Paraffin-embedded primary breast cancer samples were stained using a triple immunohistochemical method allowing simultaneous identification of carcinoma cells, macrophages, and endothelial cells. Two pathologists, blinded to outcome, evaluated the number of TMEM per 20 high-power fields.

Results: No association was seen between TMEM density and tumor size or grade, lymph node metastasis, lymphovascular invasion, or hormone receptor status. TMEM density was greater in the group of patients who developed systemic metastases compared with the patients with only localized breast cancer (median, 105 versus 50, respectively; $P = 0.00006$). For every 10-unit increase in TMEM density, the odds ratio for systemic metastasis was 1.9 (95% confidence interval, 1.1-3.4).

Conclusions: TMEM density predicted the development of systemic, hematogenous metastases. The ability of TMEM to predict distant metastasis was independent of lymph node status and other currently used prognosticators. Quantitation of TMEM may be a useful new prognostic marker for breast cancer patients.

Breast cancer is the most prevalent malignant disease of women in the developed world, apart from nonmelanoma skin cancers, with ~1 in 8 women in the United States being

diagnosed with breast cancer at some time in their lives. Breast cancer mortality is largely attributable to the development of systemic, hematogenous metastatic disease. Although ~10% to 15% of patients have an aggressive form of the disease that metastasizes within 3 years after initial diagnosis, the clinical manifestations of occult metastatic disease can appear ≥ 10 years later. The consequence is that most breast cancer patients carry a risk for development of metastatic disease throughout the remainder of their natural lives (1, 2).

To decrease the risk for the emergence of metastatic tumors, ~80% of breast cancer patients are treated with adjuvant chemotherapy. The clinical benefit is a 3% to 10% increase in 15-year survival depending on the age of the patient at diagnosis. However, because only ~40% of these patients eventually relapse and develop metastatic disease, there is a significant subset of patients who are unnecessarily subjected to the acute and long-term side effects of current chemotherapeutic regimens (1). Currently established clinical prognostic criteria such as the histopathologic grade of the tumor or tumor size do not successfully predict systemic metastatic potential. Even angiolymphatic invasion and the presence of regional lymph node metastases do not always correlate with subsequent distant spread. This may be because the mechanisms of hematogenous spread are different from those for

Authors' Affiliations: ¹Department of Pathology and Laboratory Medicine, Weill Cornell Medical College, New York, New York; ²Department of Epidemiology and Population Health, and ³Department of Anatomy and Structural Biology, Program in Tumor Microenvironment and Metastasis, Albert Einstein Cancer Center, Albert Einstein College of Medicine, Bronx, New York; and ⁴Department of Biology, Koch Institute for Integrative Cancer Biology, Massachusetts Institute of Technology, Boston, Massachusetts

Received 8/19/08; revised 12/2/08; accepted 12/5/08; published OnlineFirst 3/24/09.

Grant support: NIH grants CA100324 (T.E. Rohan), CA113395 (J.S. Condeelis), and GM58801 (F.B. Gertler) and Integrative Cancer Biology Program grant 1-U54-CA112967 (F.B. Gertler).

The costs of publication of this article were defrayed in part by the payment of page charges. This article must therefore be hereby marked *advertisement* in accordance with 18 U.S.C. Section 1734 solely to indicate this fact.

Note: Supplementary data for this article are available at Clinical Cancer Research Online (<http://clincancerres.aacrjournals.org/>).

Requests for reprints: Joan G. Jones, Department of Pathology and Laboratory Medicine, Weill Cornell Medical College, 525 East 68th Street, Starr-1015D, New York, NY 10065. Phone: 212-746-6328; Fax: 212-746-0465; E-mail: joj2013@med.cornell.edu.

© 2009 American Association for Cancer Research.
doi:10.1158/1078-0432.CCR-08-2179

Translational Relevance

Multiphoton-based intravital imaging has shown that invasive carcinoma cells in mouse and rat mammary tumors intravasate when associated with perivascular macrophages. To identify this microenvironment in human breast cancer samples, we have developed a triple immunostain that simultaneously labels invasive carcinoma cells, macrophages, and endothelial cells. We call the direct apposition of these three cell types "TMEM" (tumor microenvironment of metastasis). In this study, we confirm that TMEM are present in human breast cancer specimens and can be identified in routine histologic sections. Additionally, we found that TMEM density is associated with the development of distant organ metastasis independent of lymph node status and tumor grade. TMEM may be a novel and useful marker for predicting the development of systemic, hematogenous metastasis in breast cancer patients.

lymphatic spread. The ability to identify at the time of diagnosis those tumors that have increased likelihood for systemic hematogenous spread would aid in tailoring therapeutic interventions specific for a particular patient and in identifying those patients who would benefit the most from systemic therapy.

We have shown previously that in rodent models the tumor microenvironment is critical in the facilitation of metastasis. Using intravital multiphoton imaging in rat and mouse mammary tumors, invasive carcinoma cells have been shown to polarize, move toward, and invade blood vessels (3). This polarization and increased motility, leading to invasion of blood vessels by carcinoma cells, requires a paracrine loop involving macrophage-derived epidermal growth factor and carcinoma cell-derived colony-stimulating factor-1 (3, 4). Invasive carcinoma cells involved in this paracrine loop yield a distinct gene expression profile, called the invasion signature, and increased cell motility and invasion are the result of alterations in the expression of cytoskeletal regulatory proteins (5, 6).

A key actin polymerization regulatory protein that is part of the invasion signature and that is up-regulated in invasive tumor cells is Mena (5–7), an Ena/VASP protein family member that is highly conserved across species (8, 9). Mena regulates cell movement by its ability to protect actin filaments from capping proteins during polymerization (10). Mena is up-regulated in malignant human breast tumors (11–13) and is overexpressed in a subpopulation of invasive tumor cells of rat and mouse mammary tumors (5–7), suggesting that Mena plays a central role in regulating breast carcinoma cell invasion. The forced expression of Mena in tumor cells at levels observed in invasive tumor cells has shown that Mena promotes carcinoma cell motility and invasiveness both *in vivo* and *in vitro* and increases intravasation and lung metastasis *in vivo*. Mena stabilizes invadopodia, actin-rich protrusions that contain proteases, thereby increasing the matrix degradation activity of tumor cells. Importantly, Mena activity potentiates epidermal growth factor-induced carcinoma cell invasion and membrane protrusion. In aggregate, these results indicate that the up-regulation of Mena expression in invasive tumor cells enables them to invade and metastasize in response to otherwise benign epidermal

growth factor stimulus levels, thereby increasing responsiveness to macrophage signaling (14).

The density of tumor-associated macrophages has been suggested to be a prognostic marker of poor outcome for a variety of carcinomas, including breast carcinoma (15, 16). Macrophages comprise a key component of the tumor microenvironment as facilitators of tumor cell migration and intravasation, stromal matrix breakdown, and angiogenesis (16). In murine mammary tumors resulting from the expression of the *PyMT* oncogene in wild-type mice with intact macrophage numbers and function, carcinoma cells, when associated with macrophages, show an invasive phenotype with increased motility (4, 17). Tumor cell motility occurs >80% of the time in association with macrophages. Extensive multiphoton time lapse imaging of live tumors has shown that tumor cell intravasation was only observed in association with perivascular macrophages and was not seen in regions of blood vessels without perivascular macrophages. A 7-fold reduction in the number of perivascular macrophages in *Csf1^{op}/Csf1^{op}* mice was correlated with a 10-fold reduction of circulating tumor cells in the blood of the same mice. Therefore, although tumor cell intravasation in the absence of perivascular macrophages cannot be ruled out, it has not been detected *in vivo* by direct imaging and may be only a minor kinetic component of intravasation. Meanwhile, perivascular macrophage-assisted tumor cell intravasation appears to be a major portal of entry of tumor cells into the blood (3).

Based on the results with mouse mammary tumors, it is postulated that human breast tumor-associated macrophages guide carcinoma cells to blood vessels via the epidermal growth factor/colony-stimulating factor-1 paracrine loop and that Mena-overexpressing carcinoma cells in particular interact with perivascular macrophages to constitute a microanatomic landmark or portal leading to carcinoma cell intravasation. We call this microanatomic landmark composed of a perivascular macrophage in contact with a Mena-overexpressing tumor cell, the tumor microenvironment of metastasis (TMEM; Fig. 1).

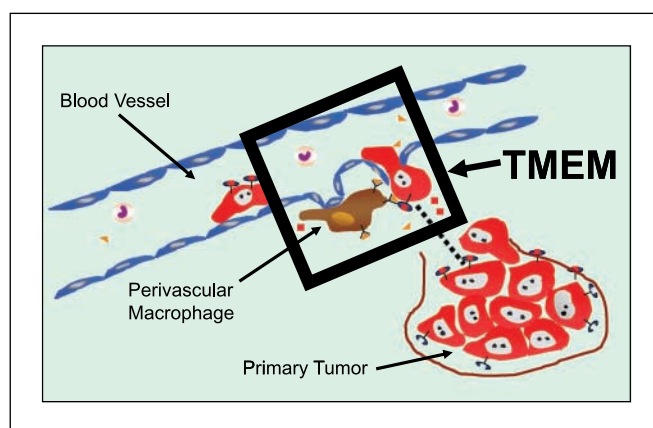
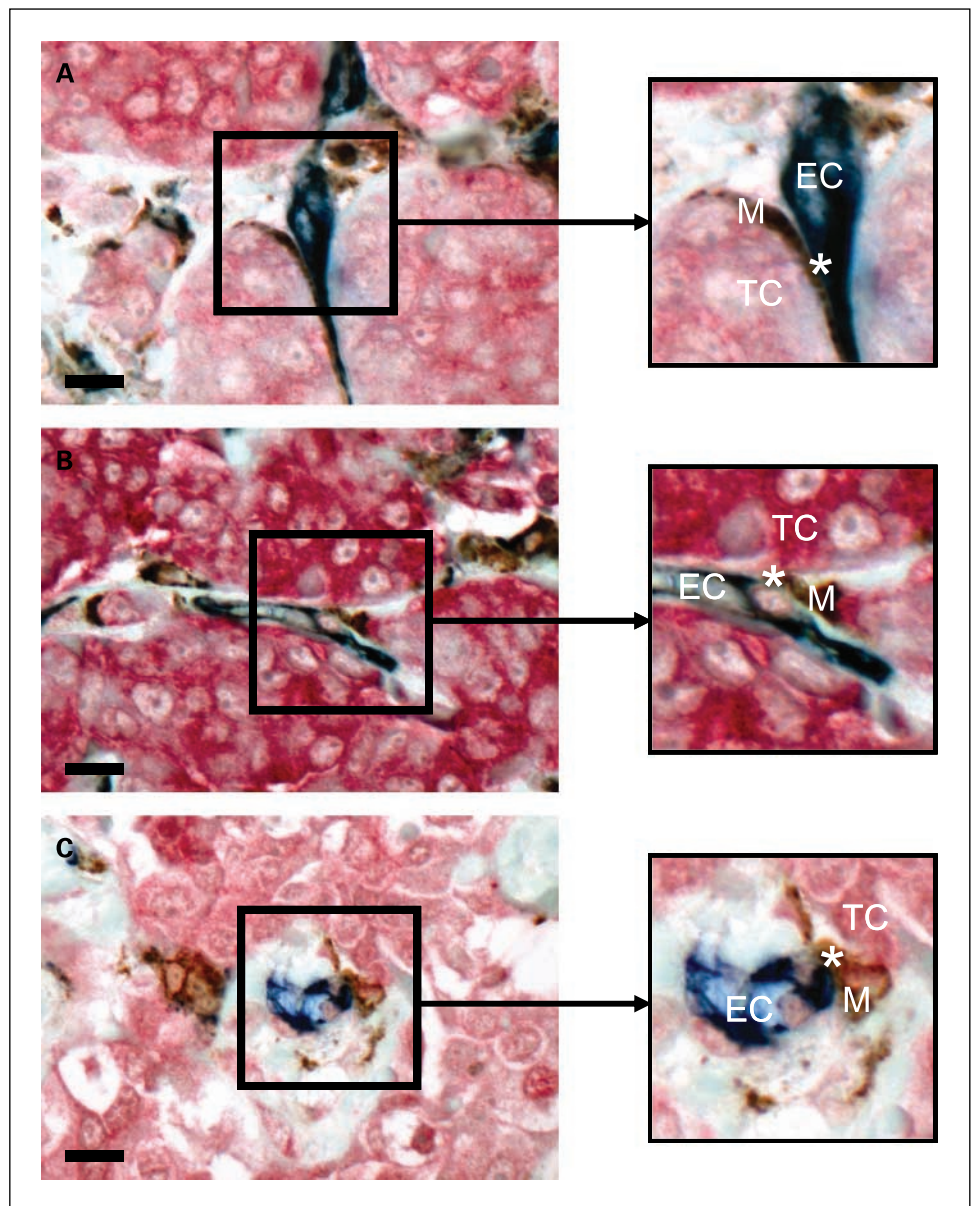


Fig. 1. Definition of TMEM. Cartoon depicting findings in rat and mouse mammary tumors where tumor cells are observed to migrate to blood vessels and intravasate in association with perivascular macrophages. *Black box*, anatomic compartment where intravasation occurs, as observed in the rodent mammary tumors, and also corresponds to the areas identified and scored as TMEM in histologic sections in our study. TMEM is defined as the tripartite arrangement of a tumor cell (*red*), macrophage (*brown*), and endothelial cell (*blue*) all in direct apposition. *Dashed line*, path taken by migratory tumor cells toward perivascular macrophages, as seen *in vivo*. Box, 60 μ m on a side.

Fig. 2. Identification of TMEM in histologic sections. *A* to *C*, different examples of TMEM as scored in histologic sections. In our triple immunostain, macrophages are *brown*, endothelial cells are *blue*, and tumor cells expressing Mena are *red*. Boxes, area of TMEM, defined as the direct apposition of a perivascular macrophage and a Mena-expressing tumor cell. In the enlarged images of the boxes (*right*), the *asterisk* denotes the "epicenter" of the TMEM, where the three cell types are most intimately apposed. *A*, blood vessel courses between nests of tumor cells. At the *asterisk*, the macrophage (*M*) is interposed between the endothelial cell (*EC*) and the tumor cell (*TC*). *B*, macrophage again is seen interposed between the tumor cell and the endothelial cell at the site of the *asterisk*. *A* and *B*, vessel is seen in longitudinal section. *C*, same intimate relationship is seen among endothelial cell, macrophage, and tumor cell, but the vessel is seen in cross-section. Note that in all the examples there is no collagen seen between the three cell types. Original magnification, $\times 600$; bar, 20 μm ; boxes, 60 μm on a side.



In this study, we show that TMEM are present in explanted, human invasive breast tumors, that the density of TMEM correlates with the histologic grade of the tumors, and that TMEM density is positively associated with the risk of developing distant organ metastases.

Materials and Methods

Preliminary to assessing TMEM density in cases with known outcome, we evaluated macrophage and blood vessel density in examples of benign and malignant breast tissue and also evaluated perivascular macrophage density and TMEM density in a series of invasive ductal carcinomas without known outcome. These initial measurements were made to determine if any of the three markers used individually correlated with tumor grade, which may be used as a surrogate for clinical outcome. Thus, this study had three distinct components. Patient samples for each component

were unique, and the case composition of each part is described below along with the associated methodology. All immunohistochemical staining was done on archival, paraffin-embedded tissue obtained from the archives of the Department of Pathology and Laboratory Medicine at New York-Presbyterian Hospital/Weill Cornell Medical College and used a Bond Max Autostainer and reagents (Vision Biosystems) unless otherwise specified. The modified Bloom-Richardson grading scheme was used to determine tumor grade/differentiation in all cases. Institutional review board approval was obtained for all parts of this study.

Evaluation of macrophage and blood vessel density in benign and malignant breast tissue. Ten cases each of well, moderate, and poorly differentiated ductal carcinomas of the breast were evaluated for this part of the study. An additional 10 cases each of ductal carcinoma *in situ* (DCIS) and benign macromastic breast tissue (obtained from reduction mammoplasties) were also included for comparison. Representative sections from each case were stained using double immunohistochemistry for CD68 (macrophage specific; ref. 18) and CD31 (endothelial cell specific; ref. 19). Sections (5 μm thick) were deparaffinized and endogenous peroxidase was inactivated followed

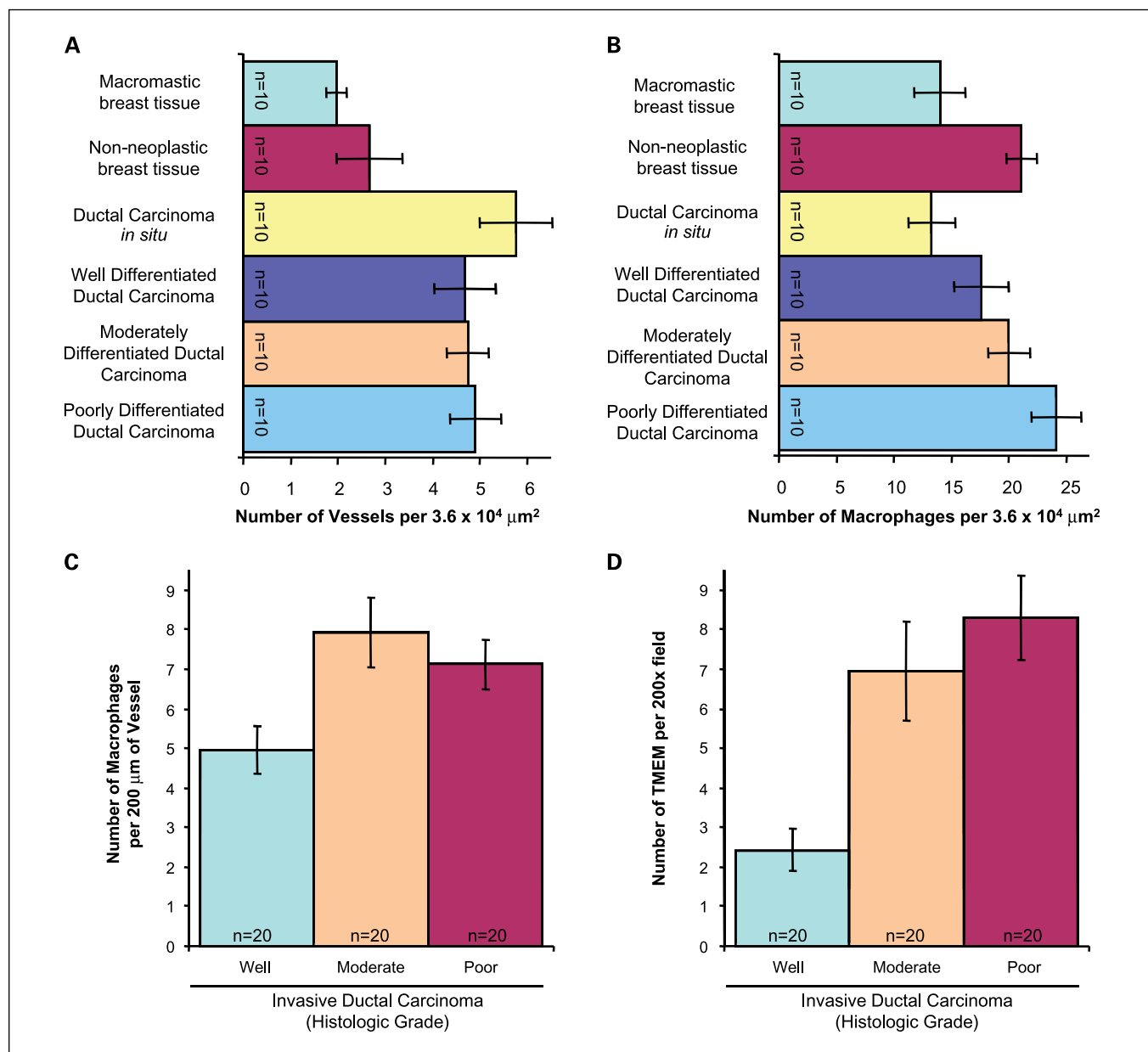


Fig. 3. Microvessel and macrophage density, perivascular macrophage density, and TMEM density in invasive ductal carcinomas. *A*, microvessel density. The density of blood vessels is higher in DCIS and invasive carcinomas than in benign breast tissue, but there is little difference in the blood vessel density among the three grades of invasive tumor. *B*, macrophage density. The density of macrophages increases from DCIS through the grades of invasive tumor, but the differences are not statistically significant and do not exceed the macrophage density of adjacent nonneoplastic breast tissue. *C*, perivascular macrophage density. Evaluating the density of macrophages along blood vessels revealed no correlation between perivascular macrophage density and tumor grade. *D*, TMEM density. TMEM counts, however, clearly separate well-differentiated from moderately ($P < 0.008$) and poorly ($P < 0.001$) differentiated carcinomas. TMEM is defined as the direct apposition of a perivascular macrophage and invasive tumor cell. Bars, SE.

by antigen retrieval with Bond Epitope Retrieval Solution 1 according to the manufacturer's instructions. CD68 was detected by incubating slides with anti-CD68 monoclonal antibody (clone PG-M1; 1:300 dilution; DAKO) followed by a polymer-based diaminobenzidine colorimetric detection system according to the manufacturer's instructions (Bond Polymer Detection Systems; Vision Biosystems). Antigen retrieval was done a second time, and slides were incubated with anti-CD31 monoclonal antibody (clone JC70A; 1:300 dilution; DAKO) and detected using an alkaline phosphatase-based streptavidin/biotinylated link system and Permanent Red chromogen (all from DAKO). Hematoxylin was used as counterstain.

Ten separate digital photographs were taken of each double immunohistochemically stained section at $\times 200$ magnification. For each picture, 10 boxes were created, each box being approximately three cell diameters across and corresponding to the hypothesized area of a TMEM. Square boxes of $60 \mu\text{m}$ on a side were chosen and centered on epithelium, as epithelial cells are necessary for the definition of TMEM. For the invasive carcinomas, an additional 10 boxes were centered on nonneoplastic epithelium adjacent to the tumor for comparison. Two pathologists (G.L.S. and J.G.J.) randomly divided all cases and independently counted and recorded the number of macrophages and blood vessels in each box. The average of the

10 boxes for each case was calculated. Differences in blood vessel density and macrophage density among the various tissue types were calculated using the Wilcoxon rank-sum test. Given that 15 comparisons were done, the *P* value for determining statistical significance was set at 0.003 by applying the Bonferroni correction to the standard assumption that *P* < 0.05 is statistically significant.

Evaluation of perivascular macrophage and TMEM densities in invasive ductal carcinomas. Twenty cases each of well, moderate, and poorly differentiated ductal carcinomas of the breast were retrieved for inclusion in this portion of the study. Representative sections of each case were stained using triple immunohistochemistry. First, sections (5 μ m thick) were deparaffinized, endogenous peroxidase was inactivated, and antigen retrieval done as described above. Next, CD68 was detected as described above. Slides were then subsequently incubated with anti-CD31 monoclonal antibody as above, except that colorimetric detection was with Vector Blue (Vector Laboratories). Finally, slides were subjected to antigen retrieval and incubated with anti-Mena monoclonal antibody (20). Detection of Mena used the Permanent Red chromogen as described above. Methylene green was used as a counterstain.

Five digital photographs of each triple immunohistochemically stained section were taken at $\times 200$ magnification (total area evaluated = 2.7 mm²). Two pathologists (B.D.R. and J.G.J.) randomly divided the cases and tabulated for all images (a) the number of perivascular macrophages along a cumulative length of 200 μ m of blood vessels and (b) the number of TMEM. The average values of these measures were then calculated for each case. Given the novelty of TMEM as a histologic entity, the two pathologists involved in scoring all cases reviewed together >200 digital images from 10 test cases stained using the triple immunohistochemical method. TMEM was defined as the direct apposition of an invasive Mena-expressing tumor cell on a perivascular macrophage. In reviewing the test cases (random archival breast cancer specimens not included in the study) and defining TMEM histologically, the two pathologists were able to achieve agreement regarding the structural variations allowed (Fig. 2). Differences in perivascular macrophage density and TMEM density among the various tissue types were calculated using the Wilcoxon rank-sum test. Given that three comparisons were done, the *P* value for determining statistical significance was set at 0.017 by applying the Bonferroni correction to the standard assumption that *P* < 0.05 is statistically significant.

Evaluation of TMEM in patients with known clinical outcome. Using the Cancer Registry at New York-Presbyterian Hospital/Weill Cornell

Medical College, 30 patients with invasive ductal carcinoma of the breast who developed systemic, distant organ metastases were identified and one control was matched individually to each case. The controls had only localized disease (invasive ductal carcinoma limited to the breast or with regional lymph node metastasis only). All patients were female and underwent primary resection of their breast cancer at New York-Presbyterian Hospital between 1992 and 2003. A minimum clinical follow-up time of 5 years was required for inclusion, and the follow-up time for all nonmetastatic patients was at least as long as that of their matched metastatic case. Due to the limited number of patients with metastatic, well-differentiated carcinomas, only patients with moderately or poorly differentiated carcinomas were included. Matching of metastatic and nonmetastatic patients was based on well-established prognostic factors including tumor grade (matched exactly), tumor size (categorized as <2, 2-4, and >4 cm), presence or absence of lymph node metastasis, and hormone receptor status.

For each patient, representative sections of tumor were subjected to triple immunohistochemical staining for CD68, CD31, and Mena as described above. In each case, 20 high-power fields ($\times 400$ magnification) were evaluated for the total number of TMEM (total area evaluated = 2.7 mm²). Two pathologists (B.D.R. and J.G.J.) each evaluated half of the cases (30 patient samples each). The cases were randomly distributed between the two pathologists, and both pathologists were blinded to the clinical outcome. After tabulation of TMEM for all samples, the cases were categorized according to whether they were metastatic and nonmetastatic, and the difference in TMEM density between metastatic and nonmetastatic patients was evaluated using the Wilcoxon signed-rank (matched pairs) test. Differences in TMEM density among other variable groups (e.g., lymph node status) were evaluated using the Wilcoxon rank-sum test. Odds ratios and 95% confidence intervals for the association between TMEM count and risk of metastasis were estimated using conditional logistic regression.

Results

Macrophage density, blood vessel density, and Mena staining are not individually correlated with tumor grade. When quantified in the four types of breast tissue examined in this study (benign macromastitic breast tissue, nonneoplastic breast tissue adjacent to carcinoma, *in situ* carcinoma, and invasive

Table 1. Clinicopathologic characteristics for the metastatic and nonmetastatic cohorts

	Metastatic (n = 30)	Nonmetastatic (n = 30)	P
Age at diagnosis (y), mean (range)	53.1 (29-88)	52.6 (30-81)	NS
Tumor grade, n (%)			
Moderate	12 (40)	12 (40)	NS
Poor	18 (60)	18 (60)	NS
Tumor size (cm), mean (range)	3.5 (1-11)	3.7 (1-10)	NS
Lymph node metastasis, present, n (%)	20 (67)	19 (63)	NS
No. lymph nodes positive, mean (range)	4.7 (0-17)	4.3 (0-14)	NS
Lymphovascular invasion, present, n (%)	18 (60)	11 (37)	NS
Hormone status, n (%)			
Estrogen receptor-positive	19 (63)	18 (60)	NS
Progesterone receptor-positive	11 (37)	15 (50)	NS
HER-2/ <i>neu</i> overexpression, present, n (%)	9 (30)	7 (23)	NS

NOTE: A search of the Cancer Registry database of the New York-Presbyterian Hospital/Weill Cornell Medical Center from 1992 to 2003 yielded 30 patients with known metastatic disease who had undergone primary resection of their breast cancer at New York-Presbyterian Hospital. The same database was then searched to identify a matched nonmetastatic control for each metastatic case. The controls were matched for each of the parameters listed above. There was a minimum follow-up time of 5 y for all cases, and the follow-up time for each control was at least as long as the follow-up time for its metastatic pair.

Abbreviation: NS, not significant; *P* > 0.05.

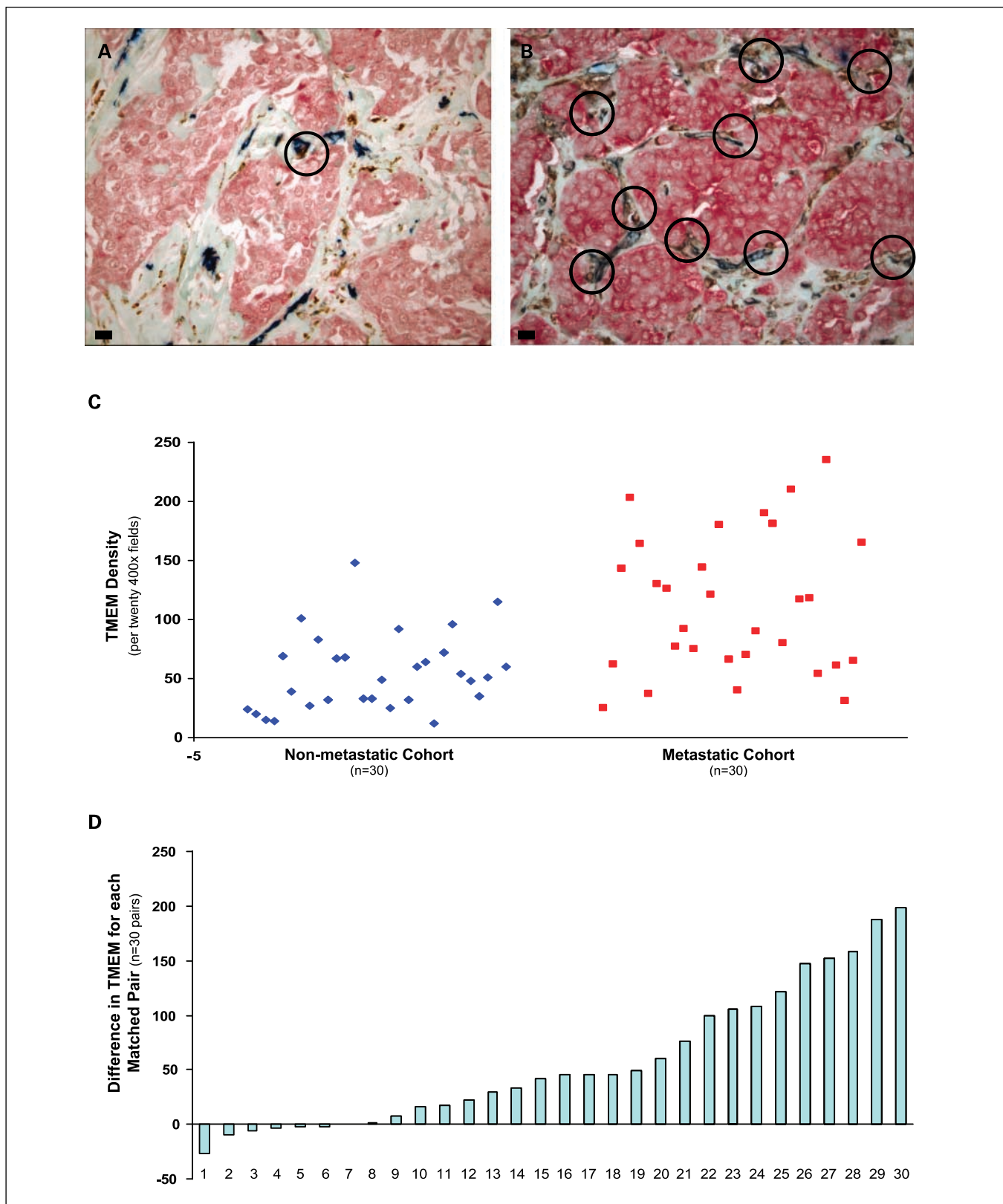


Fig. 4. TMEM density in metastatic and nonmetastatic patients. Both tumors in *A* and *B* are of similar histologic grade and are shown using the triple immunostain described previously. *A*, example of a nonmetastatic case, where TMEM counts (*circles*) tend to be low. *B*, from a patient who developed distant organ metastases, and the TMEM density is high. Although the cases in *A* and *B* are at the extreme of low and high TMEM density, we have included them for comparison given their strikingly similar histology yet disparate TMEM counts, which reinforces the novelty and utility of our triple immunostain in identifying TMEM. *C*, scatter plot depicting the TMEM counts for each of the 60 patients included in the case-control study. *D*, difference between metastatic and nonmetastatic TMEM values for each of the 30 individually matched pairs. Original magnification, $\times 400$; bar, 20 μm ; circles, 60 μm in diameter.

Table 2. Case-control study results

(A) TMEM density			
	Metastatic cohort (n = 30)	Nonmetastatic cohort (n = 30)	P
Median (5th percentile, 95th percentile)	105 (28.3, 221)	50 (13.1, 130)	0.00006
(B) Increase in risk of metastasis per 10-unit increase in TMEM			
Adjusted for	Odds ratio (95% confidence interval)		
(Unadjusted)	1.9 (1.1-3.4)		
Age at diagnosis	1.9 (1.1-3.4)		
Tumor grade	1.9 (1.1-3.4)		
Tumor size	1.9 (1.1-3.3)		
Lymphovascular invasion	1.5 (0.95-2.3)		
Lymph node metastasis	1.9 (1.0-3.6)		
Estrogen receptor status	2.0 (1.1-3.7)		
Progesterone receptor status	1.9 (1.0-3.6)		
HER-2/ <i>neu</i> status	2.2 (1.1-4.7)		

NOTE: TMEM density was significantly higher in the group of patients who developed distant metastasis compared with those with localized breast cancer (A). Additionally, for every 10-unit increase in TMEM, the odds of metastasis almost doubled (B). This estimate was robust to adjustment (separately) for the commonly used prognostic criteria listed in the table, including tumor grade, emphasizing that TMEM is not a surrogate for grade and may be a useful new independent prognostic factor.

carcinomas), neither blood vessel nor macrophage density alone were good discriminators of benign from malignant breast tissue and did not vary substantially by tumor grade. Vessel counts overall were higher in the *in situ* and invasive tumors, but vessel density was similar in all three tumor grades (Fig. 3A). Regarding vessel density, the only statistically significant differences were between macromastic breast tissue and DCIS ($P < 0.001$), macromastic breast tissue and moderately differentiated carcinoma ($P < 0.001$), and macromastic breast tissue and poorly differentiated carcinoma ($P < 0.001$). Macrophage density appeared to increase from *in situ* to invasive tumor and with increased histologic grade but did not exceed the macrophage density of nonneoplastic breast tissue adjacent to tumor (Fig. 3B). Regarding macrophage density, the only statistically significant difference was between DCIS and poorly differentiated carcinoma ($P < 0.003$).

Additionally, perivascular macrophage density was also not associated with tumor grade. As evident in Fig. 3C, the number of macrophages along a blood vessel was not significantly different among the three grades of invasive tumor ($P > 0.02$ for all comparisons).

We found that Mena was generally expressed only at low levels, if at all, in nonneoplastic ducts and lobules. All carcinoma cells, both *in situ* and invasive, showed increased Mena expression using the pan-Mena antibody (Supplementary Fig. S1). Using standard immunohistochemical methods, we could not identify patterns of subcellular localization of Mena (e.g., lamellopodia).

Identification of TMEM in histologic sections. Figure 2 provides illustrations of TMEM as seen in paraffin-embedded, immunohistochemically stained tissue sections. By definition, to qualify as a TMEM, an endothelial cell, a macrophage, and an invasive tumor cell must be in direct apposition. In our triple immunostain, the tumor cells expressing Mena are red, the endothelial cells are blue, and the macrophages are brown. All of the stains are cytoplasmic. Endothelial cells often stain with a smooth linear quality, whereas the macrophages typically show a more granular staining pattern. At low power,

if a tumor contains an abundance of collagen and is relatively avascular, the TMEM count is likely to be low. Alternatively, if one sees vessels coursing through nests of tumor cells, high-power examination may reveal macrophages in apposition to these vessels and tumor cells, thus qualifying as TMEM. As the various panels of Fig. 2 show, vessels may be cut longitudinally or in cross-section. If we found collagen fibers present between a perivascular macrophage and the tumor cells, TMEM was not scored. Additionally, if the endothelial cells and macrophages were not apposed, the definition of TMEM was also not met. Another observation was that TMEM were not localized preferentially to the central or peripheral aspects of the tumor. Rather, they were distributed uniformly across an entire tumor. Typically, they were found as single structures scattered throughout the carcinoma. In tumors that contained "hot spots" or clusters of TMEM along a single vessel, the overall TMEM counts were high.

TMEM counts are associated with tumor grade. The number of TMEM in the well-differentiated tumors was significantly lower than those in moderately and poorly differentiated tumors ($P < 0.008$ and $P < 0.001$, respectively; Fig. 3D). What was frequently observed in well-differentiated tumors was a total lack of endothelial cells in any proximity to either tumor cells or macrophages. In these fields, the TMEM score was zero. Within the moderately and poorly differentiated groups, however, there was a range in the numbers of TMEM identified, and the differences in TMEM counts between these two groups was not significant ($P > 0.02$).

TMEM density in patients with known clinical outcome. The clinicopathologic characteristics for the metastatic and nonmetastatic patients in the case-control study are presented in Table 1. Each paired metastatic and nonmetastatic patient was matched as closely as possible for the parameters listed; as such, differences between the two groups with respect to these characteristics are not statistically significant.

Figure 4A is a representative image from a nonmetastatic patient, whereas Fig. 4B depicts a representative image from a patient who developed systemic metastasis. In both images,

TMEM are denoted by circles. The individual TMEM densities for all 60 patients are depicted in Fig. 4C as a scatter plot. In Fig. 4D, each of the 30 matched pairs is considered separately, and the difference between individual metastatic and non-metastatic pairings is shown. The median (5th percentile, 95th percentile) difference between the metastatic cases and their matched nonmetastatic controls with respect to TMEM score was 43.5 (-17.1, 192), indicating that, in general, the metastatic cases had substantially higher TMEM scores than their matched controls.

TMEM density was significantly greater in the group of breast cancer patients who developed distant organ metastases compared with those with only localized disease (median, 105 versus 50, respectively; $P = 0.00006$; Table 2A). For every 10-unit increase in the TMEM count, the odds ratio for systemic metastasis was 1.9 (95% confidence interval, 1.1-3.4). This estimate was robust to adjustment (separately) for age at diagnosis, tumor grade, tumor size, lymphovascular invasion, number of lymph nodes containing metastatic carcinoma, estrogen receptor status, progesterone receptor status, and HER-2/*neu* status (Table 2B). In this limited sample, TMEM densities within each cohort (metastatic and nonmetastatic) did not differ significantly for each prognostic subgroup (Supplementary Table S1).

Discussion

Although the major cause of mortality in breast cancer is hematogenous metastasis, there are currently no reliable methodologies to predict the risk for metastatic disease. Animal studies, however, may provide some insight. Intravital imaging of invasive tumor cell behavior in mammary tumors in rats and mice has revealed a direct role for macrophages in tumor cell invasion and intravasation (3, 4). High-resolution two-photon imaging of the interactions between perivascular macrophages and tumor cells during intravasation in mouse models of metastatic mammary carcinoma has revealed the presence of a microanatomic compartment that defines the site where intravasation by motile carcinoma cells occurs. We refer to this compartment as TMEM. The constituent cells of TMEM are an endothelial cell, a perivascular macrophage, and an invasive Mena-expressing tumor cell. Mena, a member of the Ena/VASP protein family, has been identified as an up-regulated gene in the invasive migratory subpopulation of tumor cells in animal models of breast cancer (5, 6). Mena has been shown to regulate actin-driven cellular protrusions and cell motility in a variety of cell types (4, 7-10, 14), to be up-regulated in circulating tumor cells (7) and primary human breast cancers (11, 12), and to sensitize tumor cells to epidermal growth factor signals and increase metastasis (14). Hence, Mena has been postulated to be a marker for invasive, migratory tumor cells and metastatic potential (7, 14).

In our initial studies, we used tumor grade as a surrogate for prognosis (including metastasis) and asked if the individual components of TMEM alone could be predictive of poor outcome. To evaluate these components, we looked at invasive tumor cells expressing Mena, blood vessel density, and macrophage density. In our study, Mena expression was higher in tumors compared with benign epithelial cells but did not differ among the three grades of invasive carcinoma. With regard

to macrophage and blood vessel density, although there are studies on human breast cancer suggesting an association between increased densities and poor outcome (3, 16), the significance of these counts as independent predictors has not been clearly shown. A link between macrophage density and poor prognosis, for example, may be evident only in the context of other currently accepted and more frequently used prognostic markers, such as lymph node metastasis, tumor grade, and hormone receptor status (21). Similarly, when microvessel density is associated with prognosis, it is also in the context of tumor grade and lymphovascular invasion (22, 23). Our study found that microvessel density was generally elevated in the carcinomas compared with benign breast tissue, but this observation was not statistically significant, perhaps reflecting the relatively small sample size. Additionally, increasing blood vessel density was not significantly associated with increasing tumor grade. Macrophage density also tended to increase with tumor grade, but this trend again was not statistically significant.

Because tumor cells in *in vivo* animal models show greatest motility and intravasation in association with perivascular macrophages (3-5), we next assessed whether perivascular macrophage density might correlate better with tumor grade. What we found, however, was that the number of macrophages along a blood vessel, at least in invasive carcinomas, appears to be relatively constant regardless of grade.

Given the above results, then, we concluded that the individual components of our proposed microenvironment (microvessel density, macrophage density, and Mena expression) and one relational component (perivascular macrophage density) were not associated with tumor grade and therefore not likely to be of prognostic benefit.

When we looked at all the components together, however, the results were more suggestive of an association with risk of tumor progression. Defining TMEM as a perivascular macrophage in direct apposition to a Mena-expressing tumor cell, we found that TMEM counts differed significantly between well versus moderately and poorly differentiated tumors. In well-differentiated tumors, where the outcome is generally good, the TMEM count was low. In moderately and poorly differentiated tumors, there was a wide range in TMEM counts, but overall the TMEM counts were much higher than in the well-differentiated tumors. Because grade is only a surrogate for metastatic risk, finding a range is not surprising. Some moderately and poorly differentiated tumors metastasize, whereas others do not. However, very few well-differentiated tumors metastasize. In this group, not only were the overall TMEM counts low, but also the range of counts was small.

For completeness, we also looked at the staining patterns for Mena, macrophages, and endothelial cells in DCIS and nonneoplastic breast tissue. Not surprisingly, we found no TMEM in either tissue type. In benign breast tissue, there are no cancer cells, and in DCIS, the cells are noninvasive. The epithelial cells of DCIS and benign breast tissue are physically unable to appose perivascular macrophages due to an intact basement membrane as well as a layer of myoepithelial cells.

In the animal models, intravasation of tumor cells observed by direct imaging requires the direct interaction between invasive tumor cells and perivascular macrophages through a paracrine signaling loop (3, 4), and the presence of this microanatomic compartment is associated with the presence of intravascular tumor cell burden and metastasis

(3). In our study of human breast cancer samples, then, the next step was to evaluate TMEM in a case-control study of metastatic and nonmetastatic breast cancers. We identified 30 breast cancer patients with known distant metastases and 30 individually matched patients with breast cancer who had not developed metastasis from hematogenous spread. Using the same immunohistochemical triple stain, TMEM were quantified in the same fashion as for the case series of well, moderate, and poorly differentiated tumors. Well-differentiated tumors were not included due to lack of availability of metastatic samples (only two cases identified). For the series of matched pairs of moderately and poorly differentiated tumors, the difference in TMEM counts between metastatic and nonmetastatic tumors was substantial (median, 105 versus 50, respectively; $P = 0.00006$). Our results indicate that TMEM density at initial cancer resection was associated with risk of metastasis. Specifically, for an increase in the TMEM count of 10, the odds of metastasis nearly doubled. The ability of TMEM density to predict systemic spread of carcinoma cells was independent of other currently used prognosticators, including lymph node metastasis, tumor size, presence of lymphovascular invasion, and tumor grade,

although the sample size for this study precluded simultaneous adjustment for all of these factors.

Both the approach and the results in this study are novel. To date, no method for predicting metastatic risk exists that draws on the *in vivo* observation of hematogenous metastasis in animal models. These results suggest that the mechanism of hematogenous dissemination in humans is likely similar to that seen in rodent models where tumor cells intravasate in association with perivascular macrophages. A next step will be to validate these findings in a larger, independent population-based patient series with known outcome. If our results are substantiated, TMEM may be a powerful addition to the current approach for assessing metastatic risk and the need for systemic chemotherapy. If patients can be better classified as either low-risk or high-risk for metastasis, customized (patient-tailored) therapies can be designed to prevent overtreatment and undertreatment of patients, respectively.

Disclosure of Potential Conflicts of Interest

No potential conflicts of interest were disclosed.

References

- Weigelt B, Peterse JL, van't Veer LJ. Breast cancer metastasis: markers and models. *Nat Rev Cancer* 2005; 5:591–602.
- Ries LAG, Melbert D, Krapcho M, et al., editors. SEER cancer statistics review, 1975-2004. Bethesda (MD): National Cancer Institute; 2007. Available from: <http://seer.cancer.gov/csr/19752004/>, based on November 2006 SEER data submission, posted to the SEER Web site.
- Wyckoff JB, Wang Y, Lin EY, et al. Direct visualization of macrophage-assisted tumor cell motility and intravasation in mammary tumors. *Cancer Res* 2007;67: 2649–56.
- Wyckoff J, Wang W, Lin EY, et al. A paracrine loop between tumor cells and macrophages is required for tumor cell migration in mammary tumors. *Cancer Res* 2004;64:7022–9.
- Wang W, Goswami S, Lapidus K, et al. Identification and testing of a gene expression signature of invasive carcinoma cells within primary mammary tumors. *Cancer Res* 2004;64:8585–94.
- Wang W, Wyckoff JB, Goswami S, et al. Coordinated regulation of pathways for enhanced cell motility and chemotaxis is conserved in rat and mouse mammary tumors. *Cancer Res* 2007;67:3505–11.
- Goswami S, Philippar U, Wang W, et al. Identification of invasion-specific splice variants of the cytoskeletal protein Mena in mammary tumor cells. *Clin Exp Metastasis* 2009;26:153–9.
- Gertler FB, Niebuhr K, Reinhard M, Wehland J, Soriano P. Mena, a relative of VASP and *Drosophila* Enabled, is implicated in the control of microfilament dynamics. *Cell* 1996;87:227–39.
- Krause M, Dent EW, Bear JE, Loureiro JJ, Gertler FB. Ena/VASP proteins: regulators of the actin cytoskeleton and cell migration. *Annu Rev Cell Dev Biol* 2003; 19:541–64.
- Barzik M, Kotova TI, Higgs HN, et al. Ena/VASP proteins enhance actin polymerization in the presence of barbed end capping proteins. *J Biol Chem* 2005;280: 28653–62.
- Di Modugno F, Bronzi G, Scanlan MJ, et al. Human Mena protein, a serex-defined antigen overexpressed in breast cancer eliciting both humoral and CD8⁺ T-cell immune response. *Int J Cancer* 2004;109: 909–18.
- Di Modugno F, Mottolese M, Di Benedetto A, et al. The cytoskeleton regulatory protein hMena (ENAH) is overexpressed in human benign breast lesions with high risk of transformation and human epidermal growth factor receptor-2-positive/hormonal receptor-negative tumors. *Clin Cancer Res* 2006;12:1470–8.
- Di Modugno F, DeMonte L, Balsamo M, et al. Molecular cloning of hMena (ENAH) and its splice variant hMena+11a: epidermal growth factor increases their expression and stimulates hMena+11a phosphorylation in breast cancer cell lines. *Cancer Res* 2007;67: 2657–65.
- Philippar U, Roussos ET, Oser M, et al. A Mena invasion isoform potentiates EGF-induced carcinoma cell invasion and metastasis. *Dev Cell* 2008;15:813–28.
- Bingle L, Brown NJ, Lewis CE. The role of tumour-associated macrophages in tumour progression: implications for new anticancer therapies. *J Pathol* 2002;196:254–65.
- Condeelis J, Pollard JW. Macrophages: obligate partners for tumor cell migration, invasion, and metastasis. *Cell* 2006;124:263–6.
- Lin EY, Nguyen AV, Russell RG, Pollard JW. Colony-stimulating factor 1 promotes progression of mammary tumors to malignancy. *J Exp Med* 2001;193: 727–40.
- Falini B, Flenghi L, Pileri S, et al. PG-M1: a new monoclonal antibody directed against a fixative-resistant epitope on the macrophage-restricted form of the CD68 molecule. *Am J Pathol* 1993;142:1359–72.
- Parums DV, Cordell JL, Micklem K, Heryet AR, Gatter KC, Mason DY. JC70A: a new monoclonal antibody that detects vascular endothelium associated antigen on routinely processed tissue sections. *J Clin Pathol* 1990;43:752–7.
- Lebrand C, Dent EW, Strasser GA, et al. Critical role of Ena/VASP proteins for filopodia formation in neurons and in function downstream of netrin-1. *Neuron* 2004;42:37–49.
- Tsutsui S, Yasuda K, Suzuki K, Tahara K, Higashi H, Era S. Macrophage infiltration and its prognostic implications in breast cancer: the relationship with VEGF expression and microvessel density. *Oncol Rep* 2005;14:425–31.
- Dhakal HP, Naume B, Synnestvedt M, et al. Vascularization in primary breast carcinomas: its prognostic significance and relationship with tumor cell dissemination. *Clin Cancer Res* 2008;14:2341–50.
- Hansen S, Sorensen FB, Vach W, Grabau DA, Bak M, Rose C. Microvessel density compared with the Chalkley count in a prognostic study of angiogenesis in breast cancer patients. *Histopathology* 2004;44: 428–36.

Clinical Cancer Research

Tumor Microenvironment of Metastasis in Human Breast Carcinoma: A Potential Prognostic Marker Linked to Hematogenous Dissemination

Brian D. Robinson, Gabriel L. Sica, Yi-Fang Liu, et al.

Clin Cancer Res 2009;15:2433-2441.

Updated version	Access the most recent version of this article at: http://clincancerres.aacrjournals.org/content/15/7/2433
Supplementary Material	Access the most recent supplemental material at: http://clincancerres.aacrjournals.org/content/suppl/2009/03/24/1078-0432.CCR-08-2179.DC1

Cited articles	This article cites 22 articles, 10 of which you can access for free at: http://clincancerres.aacrjournals.org/content/15/7/2433.full#ref-list-1
Citing articles	This article has been cited by 39 HighWire-hosted articles. Access the articles at: http://clincancerres.aacrjournals.org/content/15/7/2433.full#related-urls

E-mail alerts	Sign up to receive free email-alerts related to this article or journal.
Reprints and Subscriptions	To order reprints of this article or to subscribe to the journal, contact the AACR Publications Department at pubs@aacr.org .
Permissions	To request permission to re-use all or part of this article, use this link http://clincancerres.aacrjournals.org/content/15/7/2433 . Click on "Request Permissions" which will take you to the Copyright Clearance Center's (CCC) Rightslink site.